

The $z_{\text{abs}} \sim z_{\text{em}}$ absorption line systems toward QSO J 2233-606 in the Hubble Deep Field South: Ne VIII $\lambda\lambda 770, 780$ absorption and partial coverage*

Patrick Petitjean^{1,2} and R. Srianand³

¹ Institut d'Astrophysique de Paris – CNRS, 98bis Boulevard Arago, F-75014 Paris, France

² UA CNRS 173 – DAEC, Observatoire de Paris-Meudon, F-92195 Meudon Cedex, France

³ IUCAA, Post Bag 4, Ganesh Khind, Pune 411 007, India

Received 24 December 1998 / Accepted 8 February 1999

Abstract. Results of a careful analysis of the highly ionized absorption systems, observed over the redshift range 2.198–2.2215 in the $z_{\text{em}} = 2.24$ HDF-S-QSO J 2233-606, are presented. The strength and covering factor of the O VI and Ne VIII absorption lines suggest that the gas is closely associated with the AGN. In addition, most of the lines show signature of partial coverage and the covering factor varies from species to species. This can be understood if the clouds cover the continuum emission region completely and only a fraction of the broad emission line region.

Using photo-ionization models we analyze in more detail the component at $z_{\text{abs}} = 2.198$, for which we can derive reliable estimates of column densities for H I and other species. Absolute abundances are close to solar but the [N/C] abundance ratio is larger than solar. This result, which is consistent with the analysis of high- z QSO broad emission-lines, confirms the physical association of the absorbing gas with the AGN. The observed column densities of N IV, N V and Ne VIII favor a two-zone model for the absorbing region where Ne VIII is predominantly produced in the highly ionized zone. It is most likely that in QSO J 2233-606, the region producing the Ne VIII absorption can not be a warm absorber.

One of the Ly α absorption lines at $z_{\text{abs}} = 2.2215$ has a flat bottom typical of saturated lines and non-zero residual intensity in the core, consistent with partial coverage. There is no metal-line from this Ly α cloud detectable in the spectrum which suggests either large chemical inhomogeneities in the gas or that the gas is very highly ionized. If the latter is true the cloud could have a total hydrogen column density consistent with that of X-ray absorbers. It is therefore of first importance to check whether or not there is an X-ray warm-absorber in front of this QSO.

Key words: galaxies: quasars: absorption lines – galaxies: quasars: individual: Q J 2233-606

1. Introduction

The QSO J 2233-606 ($z_{\text{em}} = 2.24$) has been given tremendous interest as it is located in the middle of the STIS Hubble deep field south making this field an ideal target for studying the connection between the diffuse gaseous component of the universe and galaxies (Ferguson 1998). The spectrum of this QSO shows several associated systems, (i.e. systems with $z_{\text{abs}} \simeq z_{\text{em}}$), at $z_{\text{abs}} \sim 2.2$ with broad C IV and N V absorption lines (Sealey et al. 1998, Savaglio 1998, Outram et al. 1998). HST STIS spectra, together with the available ground-based data, provide different pieces of information about these systems over the rest-wavelength range 375–2800 Å.

Associated systems have been intensively studied in the past few years because they are believed to be intimately related to the central engines of AGNs as: (i) they frequently show absorption due to high-ionization lines; (ii) they have been convincingly shown to have metallicities of the order of or above solar (Petitjean et al. 1994, Savaglio et al. 1994, Hamann 1997); (iii) the absorbing gas does not cover the background emitting region completely (Petitjean et al. 1994, Hamann et al. 1997b, Barlow & Sargent 1997). In a few cases it has been shown that the optical depth of the high-ionization lines varies with time on scales of a year (Hamann et al. 1997b) as is the case for some broad absorption line systems (e.g. Barlow et al. 1992). This requires a recombination time-scale of less than a year and hence high particle density in the absorbing gas if the observed variability is caused by the change in the ionizing conditions.

Soft X-ray spectra of an appreciable fraction of Seyfert-I galaxies show K-shell absorption edges of ionized oxygen (O VII and O VIII; Reynolds 1997, George et al. 1998). Rapid variability of these absorption edges suggests that the absorbing gas is very close to the central engine. Moreover, there is a one-to-one correspondence between the presence of associated absorption systems and X-ray “warm absorbers” in Seyfert galaxies (Crenshaw et al. 1998). The case for a unified model for X-ray

Send offprint requests to: Patrick Petitjean

* Based in part on observations obtained with the NASA/ESA Hubble Space Telescope by the Space Telescope Science Institute, which is operated by AURA, Inc., under NASA contract NAS 5–26555; observations collected at the European Southern Observatory, La Silla, Chile; and observations collected at the Anglo-Australian Observatory.

and UV absorbers, although attractive, is not completely convincing yet however. Even though Mathur et al. (1994) showed that the X-ray and UV absorptions seen in 3C351 can be reproduced by a single-cloud model, there are cases where two different ionized zones are needed even to produce the optical depth ratios of O VII and O VIII (see Reynolds 1997).

Some Seyfert-I galaxies show signatures of the existence of optically thin emitting clouds in the BLR. Shields, Ferland & Peterson (1995) have shown that the properties of the optically thin clouds in the inner BLR are consistent with that of warm absorbers (see also Porquet et al. 1998). Analysis of the broad Ne VIII $\lambda 774$ emission line in QSOs shows that the Ne VIII-emitting regions have ionization parameters in the range 5–30, total hydrogen column densities of the order of $10^{22.5} \text{ cm}^{-2}$ and average covering factors $>30\%$ for solar abundances and a nominal QSO spectrum (Hamann et al. 1998). The ionization conditions in these emitting clouds are similar to those of warm absorbers.

In order to investigate in more detail the nature of associated systems and their possible connection to warm absorbers, absorptions from species with a wide range of excitation should be studied. Moreover column densities should be determined taking into account the effect of partial coverage. In this prospect, absorption from Ne VIII, if present, is crucial as its ionization potential, 207 eV, is much higher than the ionization potential of other easily observable species. To our knowledge the Ne VIII $\lambda\lambda 770, 780$ absorption doublet has been detected in only two associated systems, in the line of sight to HS1700+6416 at $z_{\text{abs}} = 2.7126$ (Petitjean et al. 1996; see the HST spectrum in Vogel & Reimers 1995) and in the line of sight to UM675 (Hamann et al. 1995, see the spectrum in Hamann et al. 1997a) at $z_{\text{abs}} = 2.1340$. Analysis of the latter system leads the authors to conclude that, although the detection of Ne VIII provides strong evidence for a link between the associated system and the warm absorber, the total hydrogen column density in the Ne VIII phase is too small to produce the warm absorber phenomenon. Recently Telfer et al. (1998) have done a similar study (including detection of Ne VIII) of the broad absorption line system present in QSO SBS 1542+531. Note that in all previous studies Ne VIII absorption is investigated with low dispersion FOS spectra.

In the following we discuss in detail the associated systems in the line of sight to QSO J 2233-606 and especially the unambiguous detection of strong Ne VIII absorption. We briefly present the method to derive column densities in case of partial coverage in Sect. 2; describe the data in Sect. 3 and the individual absorption systems in Sect. 4, discuss the physical consequences of the observations in Sect. 5 and draw our conclusions in Sect. 6.

2. Partial coverage

When an absorbing cloud does not cover the background source completely, the observed residual intensity in the normalized spectrum, R_λ , can be written as,

$$R_\lambda = (1 - f_c) + f_c \times \exp(-\tau_\lambda), \quad (1)$$

Table 1. Spectroscopic data

Inst./Tel.	Coverage (Å)	R	S/N per pixel	Ref.
E230M-STIS/HST	2275–3118	30000	1.5–4	^a
G140L-STIS/HST	1126–1721	~ 1100	10–18	^a
G230L-STIS/HST	1585–3173	~ 550	20–45	^a
G430M-STIS/HST	3025–3565	~ 6000	5–15	^a
UCLES/AAT	3530–4390	35000	5–30	^b
EMMI/NTT	4386–8270	21000	8–10	^c

^a Ferguson (1998),

^b Outram et al. (1998),

^c Savaglio (1998)

where, τ_λ and f_c are the optical depth and covering factor respectively. The latter is the ratio of the number of photons produced by the region of the background source that is occulted by the absorbing cloud to the total number of photons (Srianand & Shankaranarayanan 1999). If two absorption lines with rest-wavelengths λ_1 and λ_2 originate from the same ion (usually it will be doublets or multiplets), their residual intensities, R_1 and R_2 , at any velocity v with respect to the centroid of the lines are related by,

$$R_2(v) = 1 - f_{c2} + f_{c2} \times \left(\frac{R_1(v) - 1 + f_{c1}}{f_{c1}} \right)^\gamma \quad (2)$$

where f_{c1} and f_{c2} are the covering factors calculated for the two lines and,

$$\gamma = \left(\frac{f_2 \lambda_2}{f_1 \lambda_1} \right)$$

with f_1 and f_2 the oscillator strengths (see e.g. Petitjean 1999). The value of γ is close to 2 for doublets.

Though our intuition says that $f_{c1} = f_{c2}$ it need not be true in general (Srianand & Shankaranarayanan 1999). Indeed due the complex velocity structure in the BLR, photons that could be absorbed by lines 1 and 2 (even in the case of doublets) originate from spatially distinct regions in the BLR. A cloud can thus be black in line 1 (covering the BLR region emitting at the corresponding wavelength λ_1), but not in line 2 if it does not cover at the same time the region emitting photons with wavelength λ_2 . Also, the interpretation of the relative covering factors for various ions is not straightforward. Indeed, the covering factor of absorption lines seen over the wavelength range of the QSO spectrum that is dominated by the continuum may be larger than the covering factor of lines present on top of the QSO emission lines as the extension of the BLR is larger than that of the continuum emission region.

3. Data

In the following analysis we use spectra of QSO J 2233-606 obtained with different instruments and telescopes. Table 1 gives the instrumentation, wavelength coverage, spectral resolution, typical signal-to-noise ratio and reference for the data available.

Ultra-violet and optical spectra were taken by the HST HDF-S STIS Team (Ferguson 1998) with the STIS E230M, G140L, G230L and G430M gratings on board the Hubble Space Telescope. Optical data was obtained at the AAT and ESO/NTT by Outram et al. (1998) and Savaglio (1998) respectively. We have corrected the data for fluctuations in the zero-level by fitting low order polynomials to the bottom of the strong saturated Ly α lines. The echelle data have been smoothed using a gaussian filter of width 3 pixels. The continuum was fit with low-order polynomials and the spectrum was normalized.

4. Description of the associated system

4.1. Overview

The absorption profiles produced by the associated absorbers are shown for the most important transitions on a velocity scale in Fig. 1. Complementary identifications in the G230L spectrum of lower quality because of the presence of the LLS break at $\sim 2700 \text{ \AA}$ are given in Fig. 2. The two spectra obtained in 1997 (end of october) and 1998 (beginning of october) are superimposed on Fig. 2 to look for variability. It can be seen that the modest signal-to-noise ratio prevents any firm conclusion about the variability of the Ne VIII absorption lines. There are absorption features near the expected position of Mg $\lambda\lambda 609,624$ but, due to poor spectral resolution, this cannot be ascertained. On the contrary, O V and probably N III are present. The maximum column density of He I found in the models discussed below is $\sim 10^{11} \text{ cm}^{-2}$. We thus do not believe that the possible line at $\sim 1875 \text{ \AA}$ seen in only one of the spectra can be He I $\lambda 584$.

The emission redshift of QSO J 2233-606, derived from the high-ionization emission lines C IV, C III] + Al III, $z_{\text{em}} = 2.237$, is smaller than the redshift derived from Mg II, $z_{\text{em}} = 2.252$, by about 1390 km s^{-1} (Sealey et al. 1998). Considering the Mg II redshift as more representative of the intrinsic redshift (Carswell et al. 1991), the associated absorptions, seen over the redshift range 2.198–2.2215, have outflow velocities relative to the quasar of $2800\text{--}5000 \text{ km s}^{-1}$ which is modest compared to usual associated or BAL outflows.

4.2. $z_{\text{abs}} = 2.2215$

There is a Ly α line at this redshift with flat bottom, consistent with line saturation, but with non-zero residual intensity. From the latter, it can be seen on Fig. 3 that the minimum covering factor for this line is $f_c \sim 0.7$. However before drawing any conclusions it is important to show that the feature is not due to blending of a few weaker lines. In Fig. 3 we plot the line profiles of the other detected Lyman series lines from this system. It can be seen that the Ly β line is very strong. Moreover the residual intensity in the Ly β line is *smaller* than the residual intensity in the Ly α line, consistent with saturation of the Ly α line.

We first assume that the covering factor is the same for Ly α and Ly β . In the middle panel we plot the observed Ly β profile together with the predicted Ly β profiles computed from the Ly α profile for three values of the covering factor: dotted, short-

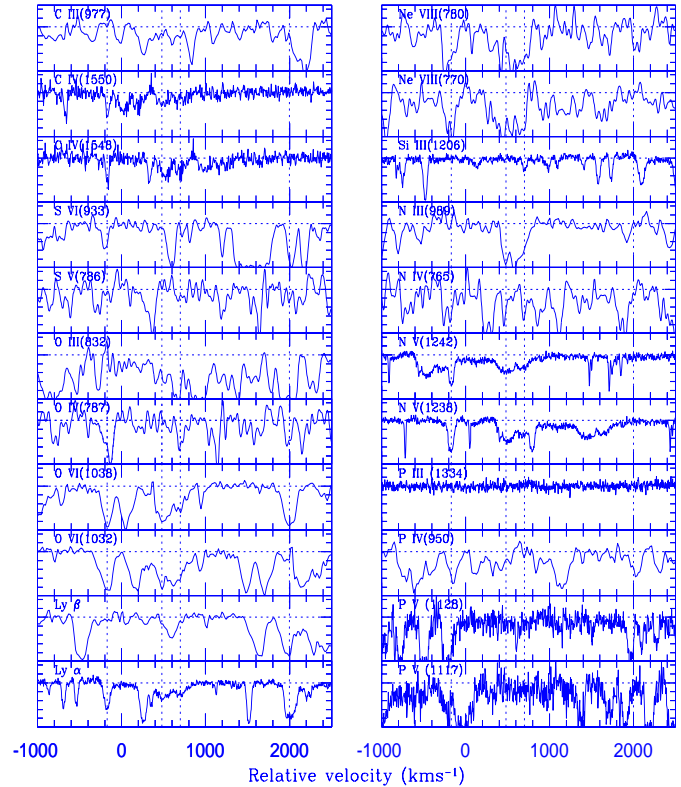


Fig. 1. Absorption profiles of different transitions in the associated systems observed along the line of sight to J 2233-606. The zero velocity is taken at $z = 2.20$. The vertical dashed lines mark redshifts 2.1982, 2.2052, 2.2075 and 2.2215 from the left to the right. Note the component at $+950 \text{ km s}^{-1}$ ($z_{\text{abs}} = 2.21$) with O VI and Ne VIII but no detectable H I absorptions.

dashed and long-dashed lines are for covering factors 1, 0.8, 0.70 respectively.

The predicted Ly β profiles are inconsistent with the observed Ly β profile and the latter seems too strong even for the minimum covering factor acceptable for the Ly α line ($f_c \sim 0.7$). The numerous saturated lines present in this part of the spectrum assures that the error in the zero level determination cannot explain the discrepancy. Although we cannot reject the presence of weak Ly α absorption lines superimposed with the Ly β absorption, especially in the blue-wing, the good wavelength coincidence between Ly β and Ly α seems to indicate that the contamination cannot be large. One way to explain the apparent strength of the Ly β line is to assume that the covering factor for Ly β is *larger* than for Ly α . Note that this is consistent with the QSO Ly α emission line to be stronger than the Ly β emission line. If true, then we can expect that the covering factor of the Ly γ line be even larger.

In the top panel we plot the observed wavelength range of the Ly γ line and the predicted profile using the Ly β profile for covering factors 1 (dotted line) and 0.9 (dashed lines). The best match is obtained for complete coverage though this does not reproduce the Ly γ very well. Smaller values of the covering factor predict too strong a Ly γ line. We conclude that, in order to

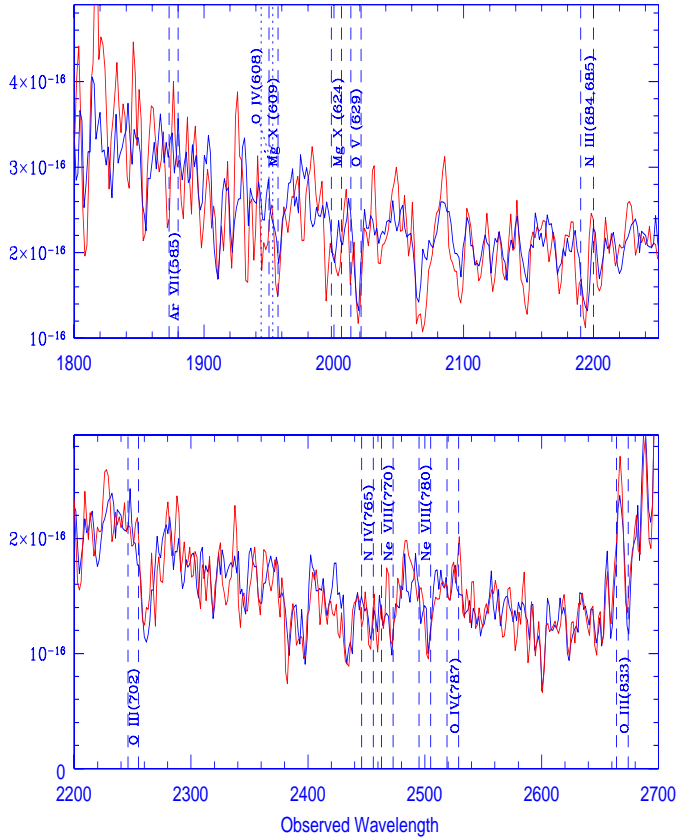


Fig. 2. Possible identifications of lines from the associated system in the G230L spectrum. The vertical dashed lines mark the redshift range 2.198–2.210. The two spectra obtained in 1997 (end of October) and 1998 (beginning of October) are superimposed to look for variability. It can be seen that the modest S/N ratio prevents any firm conclusion about the variability of the Ne VIII absorption lines.

understand the residual intensities in the different Lyman series absorption lines, it must be assumed that the covering factor increases from Ly α to Ly γ . It is thus likely that the absorbing cloud at $z_{\text{abs}} = 2.2215$ completely covers the continuum source and partially covers the BLR.

This system does not show absorption due to any detectable heavy element transitions either in the optical data (Outram et al. 1998; Savaglio 1998) or in the HST data. If partial coverage is a signature of physical association between the absorbing gas and the AGN, then the lack of metal lines in this system could suggest that there are large inhomogeneities in the chemical enrichment of the gas physically associated with central engines of QSOs. However, on the contrary, if we presume that the gas associated with the central regions of the quasar is more or less uniformly enriched, then this system could correspond to very highly ionized gas. The ionization state should be such that all observable metal transitions are weak and undetectable. This condition demands $\log \text{H I}/\text{H}$ to be smaller than -8 (e.g. Hamann 1997) and $\log N(\text{H}) > 22$. Note that such a cloud could be related to the warm absorbers.

Another possibility is that the gas is extremely metal-poor and is produced by an intervening cloud with sizes less than

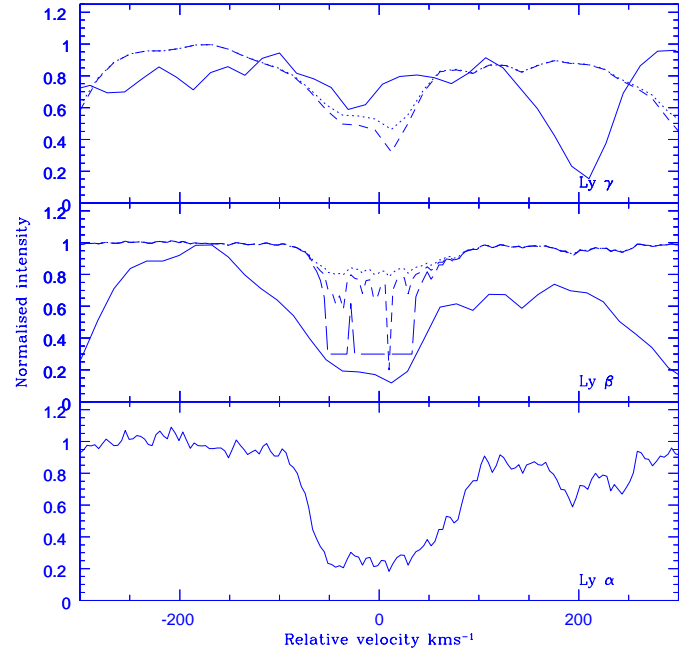


Fig. 3. Analysis of partial coverage in the $z_{\text{abs}} = 2.2215$ system. The observed Ly α profile is plotted in the bottom panel. The middle panel shows the observed Ly β profile (solid) together with the predicted profiles computed from Ly α assuming covering factors $f_c = 1, 0.8$ and 0.70 for the dotted, short-dashed and long-dashed lines respectively. The top panel shows the observed Ly γ profile with the predicted profiles computed from Ly β assuming covering factors $f_c = 1$ and 0.9 for the dotted and dashed lines respectively.

the BLR (i.e. few pc). Not only this is much smaller than the dimensions derived for intervening Ly α clouds using adjacent lines of sight (e.g. Petitjean et al. 1998) but also these clouds would have been detected by previous surveys far away from the QSO.

4.3. $z_{\text{abs}} = 2.207$

The C IV, N V and Ly α absorption lines produced by this system are shallow and broad ($\sim 500 \text{ km s}^{-1}$) like a miniaturised Broad Absorption Line system (BALs). Outram et al. (1998) discuss the N V and Ly α absorptions from this system. They could not fit the N V doublet when assuming 100% coverage. However, they managed to obtain a consistent fit after correcting the continuum by subtracting a Gaussian centered at 3938 \AA with $\text{FWHM} = 670 \text{ km s}^{-1}$ and maximum depth 19 percent of the original continuum level. They used a three-component model with large velocity dispersions. Savaglio (1998) observed the C IV absorption doublet from this system. She could fit the doublet with six components. The O VI and Ne VIII doublets are detected in the G430M and E230M spectra respectively. Note that the O VI doublet is observed at slightly lower resolution than N V and C IV and the Ne VIII doublet is found in a low S/N region blueward the Lyman limit of the moderately thick system at $z_{\text{abs}} = 1.87$. Finally, strong O V $\lambda 629$ is seen at $\sim 2020 \text{ \AA}$ as expected and possibly Mg X $\lambda 624$ at $\lambda 2000 \text{ \AA}$.

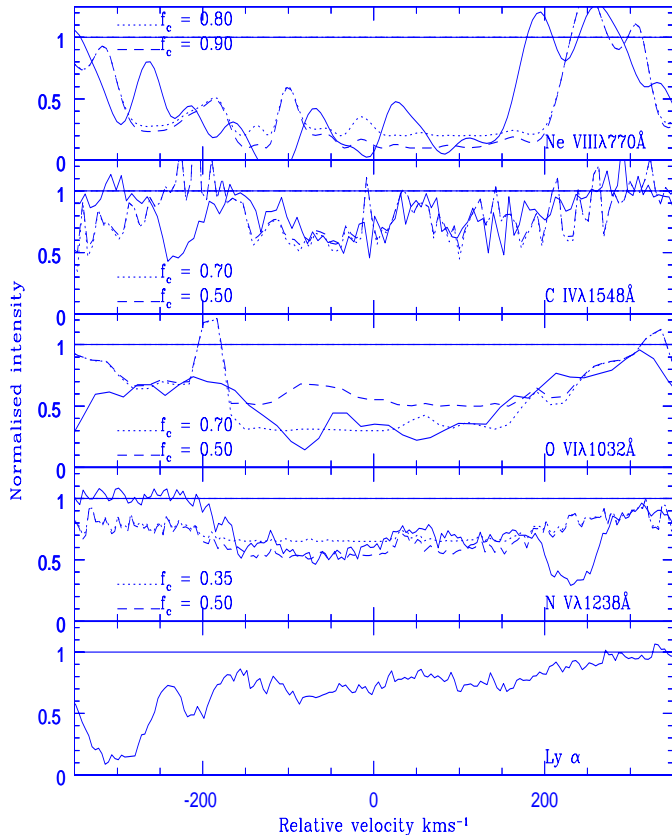


Fig. 4. Analysis of partial coverage in the $z_{\text{abs}} = 2.207$ system. The observed $\text{Ly}\alpha$ profile is plotted in the bottom panel. The solid curves in the other panels are the observed profiles of the stronger line of the doublets. The dotted and short-dashed lines are the predicted velocity profiles computed from the profile of the second transition of the doublet and assuming covering factors $f_c = 0.35$ (dotted line) and 0.50 (dashed line).

The stronger line of the C IV, N V, O VI and Ne VIII doublets, together with the $\text{Ly}\alpha$ line, are plotted on Fig. 4 on a velocity scale. The dotted and dashed lines are the predicted velocity profiles computed from the profile of the second transition of the doublets for different values of the covering factor. Here again we assume identical covering factors for both transitions. It can be seen that in order to reproduce the residual intensities of N V we need a covering factor of the order of 0.35 at $v \sim +150$ km s^{-1} and 0.50 at $v \sim -100$ km s^{-1} . The difference between the two models with $f_c = 0.35$ and 0.50 , is, at these places, of the order or larger than 0.1 (10% of the normalized continuum; see Fig. 4) when the rms deviation in the spectrum is ~ 0.04 .

The O VI profiles are consistent with a covering factor ~ 0.7 that cannot be reconciled with the values found for N V. Note that the O VI profiles could be affected by the relatively poor spectral resolution and the derived covering factors should be considered as lower limits. The maximum error in the covering factor for the O VI lines is about 0.1 , computed from the error in the residual intensity. The S/N ratio over the C IV doublet is not good enough and consistent residual intensities are obtained for a wide range of covering factors. The covering factor required

for the Ne VIII lines is in the range 0.8 – 1.0 with an error per pixel of 0.15 . The covering factor derived from the Ne VIII lines is therefore significantly larger than the one derived from the N V doublet. There seems to be an anti-correlation between the covering factor and the ionization state or the wavelength. This again is consistent with clouds partially covering the BLR while covering most of the continuum emission region.

Another interesting observation concerns the doubly-ionized species. It can be seen on Fig. 1 that O III $\lambda 832$ is certainly blended with other lines; that there may be a shallow absorption at the expected position of C III $\lambda 977$ although most of it should be $\text{Ly}\gamma$; and that there is a strong absorption at the expected position of N III $\lambda 989$. This line cannot be $\text{Ly}\beta$ at $z_{\text{abs}} = 2.093$ as there is no corresponding $\text{Ly}\alpha$ line. We cannot reject the hypothesis that this is an intervening $\text{Ly}\alpha$ line as the $\text{Ly}\beta$ range is of very poor S/N ratio. Interestingly enough, there is an absorption feature at the expected position of N III $\lambda 684,685$ (see Fig. 2). Although such a strong N III absorption would be very surprising (see next section and Fig. 6), the presence of doubly-ionized species cannot be ruled out. The corresponding absorptions from triply ionized species, although weak and noisy, could be present (see in particular O IV $\lambda 787$ and N IV $\lambda 765$). If true, this would imply that the medium has two phases of low and high-ionization (see next section).

Since the possible strong N III $\lambda 989$ line goes to zero, suggesting complete coverage; we note that there is a tendency for the absorption lines redshifted on top of the emission lines (here C IV and N V) to have covering factors smaller than lines redshifted in parts of the spectrum free from emission-lines (Ne VIII and N III). This further supports the conclusion that the gas covers the continuum emitting region but only part of the BLR.

4.4. $z_{\text{abs}} = 2.198$

$\text{Ly}\alpha$ and N V absorptions produced by this system are detected by Outram et al. (1998) who already noted the incomplete coverage of the background source. They conjectured that the absorbing cloud is larger than the continuum emitting region and smaller than the BLR. Savaglio (1998) has noted that single as well as two component fits to the C IV doublet result in a very poor fit, again suggesting partial coverage. O VI and Ne VIII doublets are detected in the HST spectra. The stronger lines of the doublets together with $\text{Ly}\alpha$ are plotted on Fig. 5 on a velocity scale. The dotted and dashed lines are the predicted velocity profiles computed from the second transition of doublets assuming different values of the covering factor (dotted, short-dashed and long-dashed lines are for $f_c = 0.7, 0.8$ and 0.9 respectively). Here again we assume identical covering factors for both transitions. The N V $\lambda 1242$ line of this system is blended with N V $\lambda 1238$ of the system at 2.208 . We have subtracted the contribution due to the N V $\lambda 1238$ line before doing the analysis. The covering factor required to fit the N V doublet is $\sim 0.7 \pm 0.04$. However the O VI profiles require values larger than 0.85 ± 0.04 . It is quite likely that the Ne VIII $\lambda 780$ is blended with some other line in the blue wing. Also the Ne VIII $\lambda 770$ profile is very noisy and is consistent with a wide range of covering factors. It is interest-

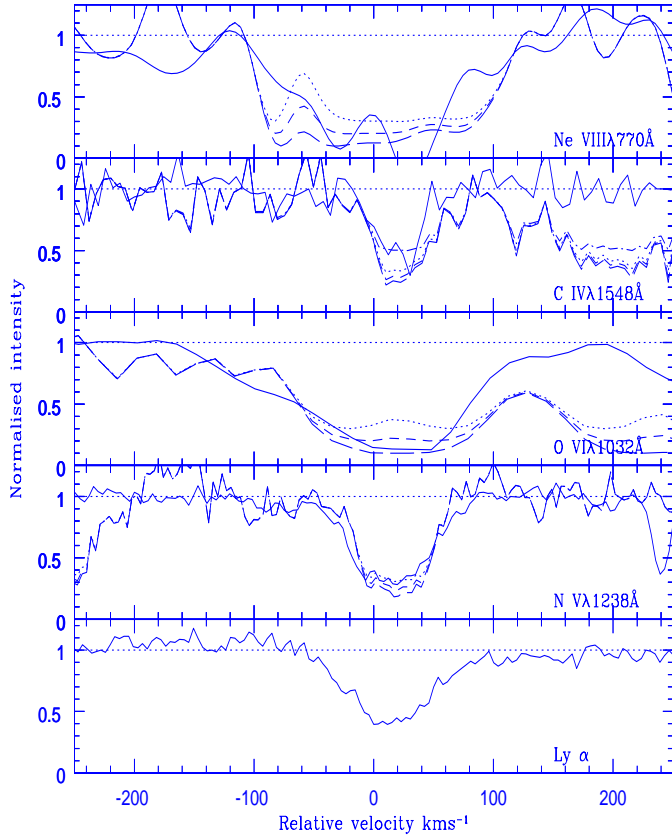


Fig. 5. Analysis of partial coverage in the $z_{\text{abs}} = 2.198$ system. The observed $\text{Ly}\alpha$ profile is plotted in the lowest panel. The solid curves in other panels are the observed profiles of the strongest transition of the doublet. The dotted, short-dashed and long-dashed lines are the predicted velocity profiles computed using the profile of the weakest member of the doublets and assuming covering factor of $f_c = 0.7, 0.8$ and 0.9 respectively.

ing to note that inspite of the poor signal to noise ratio, the C IV profiles clearly suggest that the covering factor is less than 0.7 and we have obtained a consistent fit for $f_c = 0.5$. Thus like the $z_{\text{abs}} = 2.207$ system, this system also shows different covering factor for different transitions; the covering factor being lower for C IV than for N V.

5. Physical conditions in the $z_{\text{abs}} = 2.198$ system

In this section we study the physical conditions in the $z_{\text{abs}} = 2.198$ system in greater detail. The column density per unit velocity interval at any velocity, v , with respect to the centroid of the line is given by,

$$N(v) = \frac{(m_e c / \pi e^2)}{f \lambda} \tau(v), \quad (3)$$

and from Eq. (1) the optical depth $\tau(v)$ is given by,

$$\tau(v) = -\ln \left(\frac{R(v) - 1 + f_c}{f_c} \right). \quad (4)$$

Assuming equal covering factor for the two absorption lines of a doublet, $f_{c1} = f_{c2} = f_c$, we obtain $f_c(v)$ for each doublet

using Eq. (2). We then derive the column density per unit velocity interval from Eqs. (3) and (4). The total column density, N , is obtained by integrating $N(v)$ over the velocity interval covered by the absorption line profile. For various species we give in Table 2 the absorption parameters (N and b) obtained from Voigt profile fitting (Columns 3 and 4 respectively) and the column density obtained by integration of the column density per unit velocity interval over the velocity profile (Column 7). The velocity range (Column 5), and the mean covering factor estimated over this range (Column 6) are also given. In the case of single lines we use a conservative lower limit of 0.7 for the covering factor. Note that the column density obtained with the Voigt profile fits are lower limits as corrections are not incorporated to take into account partial coverage.

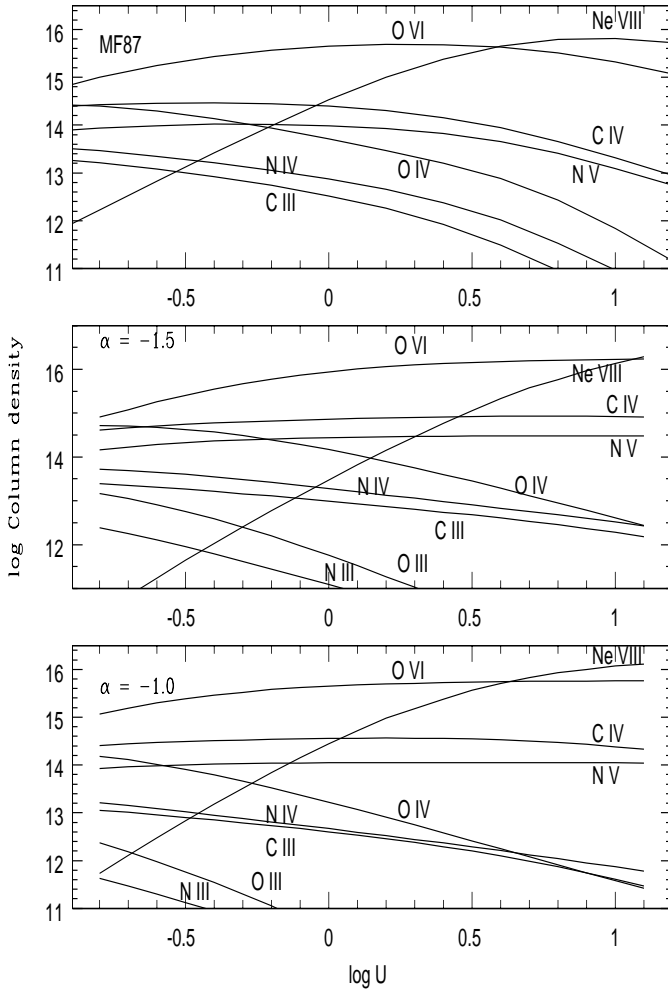
$\text{Ly}\beta$ from this system is weak and we could not derive any bound on the covering factor from the $\text{Ly}\alpha$ line only. C III $\lambda 977$ is not detected and we derive a two sigma upper limit from the continuum rms at the expected position of the line. Voigt profile fits to the C IV lines are taken from Savaglio (1998). As the estimated covering factor is low, the column density derived by fitting the profile is less by a factor of 5 compared to the estimated column density using the column density per unit velocity interval. N III and Si III are not detected whereas a line is present at the expected position of N IV $\lambda 765$. This line clearly shows two components and the blue component is clearly absent in the N V profile. The further absence of N III suggests that this component is not real. Thus we have fitted the N IV blue component as an intervening $\text{Ly}\alpha$ line and used only the column density obtained from the red component in our analysis. Although the resolution of the spectrum is not very high ($\sim 50 \text{ km s}^{-1}$), we have fitted the O VI lines using three components. There is a line at the expected position of O IV $\lambda 787$. However this line could possibly be $\text{Ly}\gamma$ from the system at $z_{\text{abs}} = 2.5907$. By carefully fitting the $\text{Ly}\alpha$, $\text{Ly}\beta$ and $\text{Ly}\delta$ lines in this system, we removed the contribution of the $\text{Ly}\gamma$ and fit the residual as O IV $\lambda 787$. As discussed before, the estimate of column densities can be somewhat uncertain due to limited S/N ratio (especially for the Ne VIII lines) and possible contamination by intervening lines.

The derived column densities for H I, C IV, N V and O VI are characteristic of associated systems (Hamann 1997). We run photo-ionization models using Cloudy (Ferland 1996) to study the ionization structure of a plane parallel cloud with neutral hydrogen column density 10^{14} cm^{-2} , solar metallicities, and illuminated by ionizing radiation fields with different spectra. Although a one-zone model is questionable in such medium, we believe that this is a reasonable representation of the absorbing cloud producing at least C IV, N V and H I (see below for O VI and Ne VIII) because the kinematics of the lines are very similar (see Figs. 1 and 5) and the partial coverages discussed in the previous sections indicate small sizes for the cloud.

Results for a typical AGN spectrum given by Mathews & Ferland (1987) and two power-law spectra are given in Fig. 6. In the framework of these models, it is apparent that the column densities are reproduced easily. The $\alpha = -1$ power-law ionizing spectrum is favored as it minimizes the $N(\text{C IV})/N(\text{O VI})$ ratio.

Table 2. Parameters for the associated system at $z_{\text{abs}}=2.198$

Ion	z	$\log N$ cm^{-2}	b (km s^{-1})	v (km s^{-1})	f_c	$\log N$ cm^{-2}
H I	2.1982	13.74 ± 0.01	43.99 ± 1.01	-47, 53	> 0.7	< 13.95
C III	< 13.40
C IV	2.1982	13.77 ± 0.05	19.80 ± 2.40	-27, 50	~ 0.5	14.48
N IV	2.1980	13.73 ± 0.04	30.43 ± 1.35		> 0.7	< 14.34
N V	2.1972	13.12 ± 0.05	32.51 ± 4.06			
	2.1982	14.57 ± 0.03	31.46 ± 0.58	-27, 53	~ 0.7	14.55
O IV	2.1979	14.43 ± 0.06	49.33 ± 2.74			
	2.1987	13.94 ± 0.08	37.70 ± 4.53	-47, 53	> 0.7	< 14.62
O VI	2.1976	14.39 ± 0.16	^a			
	2.1981	14.87 ± 0.24	^a			
	2.1987	14.63 ± 0.14	^a	-46, 100	~ 0.8	15.38
Ne VIII	2.1976	14.63 ± 0.27	39.11 ± 9.70			
	2.1981	14.79 ± 0.10	25.39 ± 3.85			
	2.1987	14.68 ± 0.09	32.33 ± 3.20	-27, 53	~ 0.7	15.10

^a Same as for Ne VIII

Fig. 6. The logarithm of column densities for species indicated next to each curve is given versus the logarithm of the ionization parameter for ionizing spectra as given by Mathews & Ferland (1987; top panel); or power-laws with index $\alpha = -1.5$ (middle panel) and -1 (bottom panel).

Although metallicities cannot be much less than solar (because of C IV and N V), it would be difficult to argue for metallicities much larger than solar (especially for oxygen). However, contrary to what is observed, the predicted C IV column density is always larger than that of N V. This suggests that nitrogen is over-abundant compared to carbon. It is interesting to note that the N V lines of the $z_{\text{abs}} = 2.207$ system is also stronger than the lines of C IV suggesting a similar abundance pattern. Indeed, using N V/C IV emission line ratios, Hamann & Ferland (1992) have shown that nitrogen is over-abundant by a factor of $\sim 2\text{--}9$ in high-redshift QSOs ($z \geq 2.0$). They suggested rapid star-formation models to boost the nitrogen abundance through enhanced secondary production in massive stars. Korista et al. (1996) have also noticed overabundance of nitrogen with respect to carbon and oxygen in the well-studied BAL system in Q 0226-1024. They could obtain a much better fit of the lines after taking into account the abundance pattern due to rapid star-formation. The overabundance of nitrogen with respect to oxygen and/or carbon, does not seem to be seen in every associated system however. Indeed, we have good data for the associated systems in Q 0207-003 and Q 0138-381 showing partial coverage. Although solar metallicities are needed to explain the line ratios, there is no indication of enhanced nitrogen abundance.

From the observed N V to N IV column density ratio, it can be seen that $\log U < -0.5$ (the ionization parameter U is the ratio of the ionizing photons density to the total hydrogen density). However such a value for the ionization parameter implies that the gas producing N V and N IV can not account for the observed value of the Ne VIII column density without an unrealistically large neon abundance. Another and more likely explanation is that there are two distinct regions with different ionization parameters and that Ne VIII predominantly originates from the more highly ionized region. This is supported by the fact that the Ne VIII absorption is spread over a larger velocity range than the N V and O VI absorptions. We can check that, even in that case, C III $\lambda 977$ would not be detectable. Indeed, the expected C III column density is of the order of 10^{13} cm^{-2} (see Fig. 6), thus $w_{\text{obs}}(\text{C III } \lambda 977) \sim 0.2 \text{ \AA}$ which is about twice below the detection limit at $\lambda \sim 3100 \text{ \AA}$.

Since the low-ionization region by itself can account for the observed H I and O VI column densities, the high-ionization region should have $N(\text{Ne VIII})$ much larger than $N(\text{O VI})$ which means $\log U$ larger than 0.5 and most probably 1.

If we suppose that this component is similar to warm absorbers detected by O VII and O VIII edges in the X-rays, then the condition that the optical depth of these edges are larger than 0.1 implies $\log N(\text{O VII}) > 17.55$ and $\log N(\text{O VIII}) > 18.00$. Photoionization models with solar abundances, fail to produce such high O VII and O VIII column densities for H I column densities in the range 10^{13} to 10^{14} cm^{-2} . Indeed, the ratios $\text{Ne VIII}/\text{Ne}$, $\text{O VII}/\text{O}$ and $\text{O VIII}/\text{O}$ are all maximized over the range of ionization parameters $U \sim 10\text{--}100$ (see Hamann et al. 1995) where $\log \text{HI}/\text{H} \sim -6$. For $\log N(\text{H I}) = 14$, this corresponds to $\log N(\text{H}) \sim 20$ and, assuming solar abundances, implies that $\log N(\text{O VII})$ and $\log N(\text{O VIII})$ are less than 17.

Thus, it is most likely that in QSO J 2233-606, the region producing the Ne VIII absorption can not be a warm absorber. It is thus of first importance to study the intrinsic spectral energy distribution of J 2233-606 especially in the X-rays.

6. Conclusion

We have studied the associated absorption systems ($z_{\text{abs}} \sim z_{\text{em}}$) in QSO J 2233-606, seen over the redshift range 2.198–2.2215, corresponding to outflow velocities relative to the quasar emission redshift ($z_{\text{em}} = 2.252$ from Mg II) of 2800–5000 km s⁻¹ which is modest compared to usual associated or BAL outflows.

We have shown that the Ly α line at $z_{\text{abs}} = 2.2215$ is saturated but has non-zero residual intensity. The covering factor of the gas is of the order of 0.7. This absorption system is unusual in the sense that there is no detectable metal lines. This could reveal chemical inhomogeneities in the gas or, and more likely, this absorption could correspond to very highly ionized gas from which no absorption due to heavier element can be detected. If the latter is true, the ionization factor log HI/H could be smaller than -8 and the total column density in the cloud larger than $\log N(\text{H}) = 22$. Such a cloud could be related to the warm absorbers.

Over the redshift range 2.198–2.21, conspicuous Ne VIII, O VI, C IV and N V absorptions are seen whereas the H I absorption is weak. From analysing these absorptions we conclude that (i) a two-phase medium of low and high-ionization respectively is required to explain the complete set of column densities; (ii) the abundances are close to the solar value but nitrogen is enhanced with respect to carbon; (iii) although difficult to ascertain there is a tendency for the absorption lines redshifted on top of the emission lines to have covering factors smaller than lines redshifted in parts of the spectrum free from emission-lines; this suggests that the gas covers the continuum emitting region but only part of the BLR. The component at $z_{\text{abs}} = 2.21$ (+950 km s⁻¹ on Fig. 1) is remarkable as, though conspicuous in Ne VIII and O VI, it is undetected in H I, C IV and N V. The column densities derived for this subcomponent by Voigt-profile fitting are $\log N(\text{Ne VIII}) = 14.57 \pm 0.10$; $\log N(\text{O VI}) = 14.05 \pm 0.06$ and $\log N(\text{H I}) < 13.30$, consistent with what is expected from a high-ionization zone.

Acknowledgements. We would like to thank all astronomers who have provided the data for this project and especially the HST HDF-S STIS team led by H. Ferguson. We thank the referee, Fred Hamann, for a careful reading of the manuscript.

References

- Barlow T.A., Junkkarinen V.T., Burbidge E.M., et al., 1992, ApJ 397, 81
 Barlow T.A., Sargent W.L.W., 1997, AJ 113, 136
 Carswell R.F., Mountain C.M., Robertson D.J., et al., 1991, ApJ 381, L5
 Crenshaw D.M., Kraemer S.B., Boggess A., et al., 1998, astro-ph/9812265
 Ferguson H.C., 1998, Space Telescope Science Institute Newsletter Vol. 15, No. 3, 6
 Ferland G.J., 1996, HAZY a Brief Introduction to Cloudy. Univ. Kentucky, Dept. Physics & Astron. Internal rep.
 George I.M., Turner T.J., Netzer H., et al., 1998, ApJS 114, 73
 Korista K., Hamann F., Ferguson J., Ferland G., 1996, ApJ, 461, 641
 Hamann F., 1997, ApJS 109, 279
 Hamann F., Barlow T.A., Beaver E.A., 1995, ApJ 443, 606
 Hamann F., Barlow T.A., Cohen R.D., Junkkarinen V., Burbidge E.M., 1997a, astro-ph/9704235
 Hamann F., Barlow T.A., Junkkarinen V., Burbidge E.M., 1997b, ApJ 478, 80
 Hamann F., Cohen R.D., Shields J.C., et al., 1998, ApJ 496, 761
 Hamann F., Ferland G.J., 1992, ApJ 391, L53
 Mathews W.G., Ferland G.J., 1987, ApJ 323, 456
 Mathur S., Wilkes B., Elvis M., Fiore F., 1994, ApJ 434, 493
 Outram P.J., Boyle B.J., Carswell R.F., et al., 1998, MNRAS in press (astro-ph/9809404)
 Petitjean P., 1999, In: Le Fevre O., Charlot S. (eds.) Proceedings of the Les Houches school: Formation and Evolution of Galaxies. Springer-Verlag, astro-ph/9810418
 Petitjean P., Rauch M., Carswell R.F., 1994, A&A 291, 29
 Petitjean P., Riediger R., Rauch M., 1996, A&A 307, 417
 Petitjean P., Surdej J., Smette A., et al., 1998, A&A 334, L45
 Porquet D., Dumont A.-M., Collin S., Mouchet M., 1998, astro-ph/9810333v2
 Reynolds C.S., 1997, MNRAS 286, 513
 Savaglio S., 1998, AJ 116, 1055
 Savaglio S., D'Odorico S., Møller P., 1994, A&A 281, 331
 Shields J.C., Ferland G.J., Peterson B.M., 1995, ApJ 441, 507
 Sealey M.K., Drinkwater J.M., Webb J.K., 1998, ApJ 499, L135
 Srianand, Shankaranarayanan, 1999, astro-ph/9901091
 Telfer R.C., Kriss G.A., Zheng W., Davidsen A.F., Green R., 1998, ApJ 509, 132
 Vogel S., Reimers D., 1995, A&A 294, 377